

Channel Characterization in the 5.8GHz Band in a Suburban Area

Wilyam D. T. Meza, Gláucio. L. Siqueira

Center for Telecommunications Studies – PUC - Rio de Janeiro, Brazil

wtorres@cetuc.puc-rio.br, glaucio@cetuc.puc-rio.br

Leni J. Matos

Graduate Program in Electrical and Telecommunications Engineering – UFF - Niterói, Brazil

lenijm@telecom.uff.br

Abstract— Based on signal measurements carried out in the 5.8 GHz band, which is reserved for unlicensed WiMAX in Brazil, this paper evaluates narrowband and wideband characteristics on the suburban area of Tanguá city in Rio de Janeiro State. Fading statistics, coverage and adjusted prediction model such as Hata-COST 231, SUI and UFPA were used in order to find the model that best fits the measurement data before ultimately determining that the UFPA model proved to be the best one. Temporal dispersion is studied through the delay spread and coherence band calculated from the power delay profiles obtained in the sounded channel.

Index Terms— Delay spread, fading, power delay profile, prediction models.

I. INTRODUCTION

Nowadays, the Brazilian Government develops a program known as *digital city* which provides internet access for the population through a WiMAX network with WiFi-enabled CPE's (Customer Premises Equipment). Three bands are available for WiMAX systems in Brazil: 2.4, 3.5 and 5.8 GHz. The last is an unlicensed band, for use in ISM (Instrumentation, Scientific and Medical) systems in 5.725 MHz to 5.850 MHz band, and U-NII (Unlicensed National Information Infrastructure), in the 5.150 MHz to 5.825 MHz band [1] and it was chosen for free internet in those digital cities.

Many articles deal with the signal coverage on 2.4 GHz [2]-[3] and 3.5 GHz [4]-[5] for applying in WiMAX system. However, the 5.8 GHz band is little explored. A modeling in that band was already made in an underground mine [3] and in wooded cities of Amazon region [6]. New terrain proposal for SUI model equations is provided in the 5.8 GHz band based on measurements carried out in cities of Amazon with some vegetation [7] and it will be used in this work.

It is very important to understand the channel behavior on the signal propagation in the 5.8 GHz band in environments where the digital cities are implemented. These are suburban ones, in general. Then, to reach good quality of communication it is necessary to have a complete characterization of the suburban channel in this band, which is not fully explored in the literature, and this article provides subsidies for the system planner through the parameters calculated from measurements in this channel besides on results for searching and simulation. For this, the analysis of the experimental

signal in a suburban area is made. The chosen frequency was 5.765 GHz and the fading statistics and signal dispersion are analyzed. Narrowband and wideband parameters are calculated and the signal coverage and the maximum data transmission rate that can be handled in this environment are obtained.

In Section II, the setup used for sounding the channel and the characteristics of the environment are presented. Section III deals with the narrowband characterization, including the small and large fading statistics, narrowband parameters, path loss and signal coverage to test fitness of three models, Hata-COST 231, SUI and UFPA, available for this frequency band. In Section IV, the wideband characterization and parameters as delay spread and coherence band are determined and the conclusion is given in Section V.

II. MEASUREMENT SETUP AND ENVIRONMENT

Table I presents the devices and equipment used in the sounding. Besides them, a Garmin GPS GPSmap62 and a laptop with Labview® installed are used for picking up the position data and the samples from the NI data acquisition module, respectively.

TABLE I. TRANSMITTER AND RECEIVER SPECIFICATIONS

Transmission (Tx) Equipments	Receiving (Rx) Equipments
Vector Signal Generator Anritsu MG3700A	Signature High Performance Signal Analyzer Anritsu MB2781B
Power Amplifier Minicircuits ZVE-3W-83	33 dB Low Noise Amplifier ABL0800-12-3315
17 dBi Sectorial Antenna OIW-5817P090V	Radome Omni-10 dBi Omnidirectional Antenna

On the transmitter side, Figure 1, the equipment was placed on the top of a building with coordinates S 22.73619°, W 42.71886° and the antenna was 49 m height.

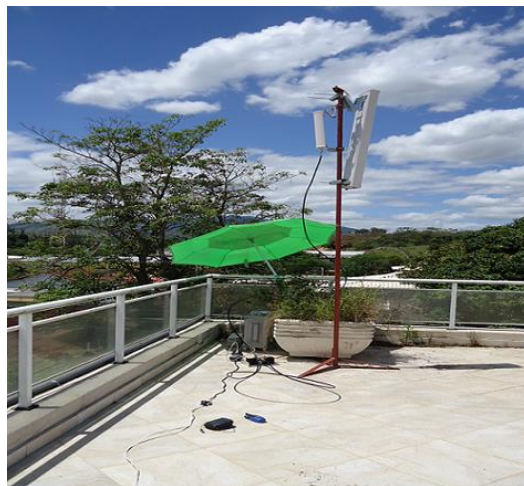


Fig. 1. Transmission setup with antenna pointing towards the city center.

The reception system, Figure 2, was mounted inside a van, with the Rx antenna on its top. The sounded area was the city of Tanguá, characterized as a suburban one with some vegetation between the residences. Eleven routes were sounded for the narrowband characterization but, in the wideband

characterization, only eight routes have had signal levels above the noise threshold and they are referred in the Section IV. Figure 3 shows all routes into the city environment. Figure 4 presents the Route 1 and the Route 2 with graduation color signal level.



Fig. 2. Mobile Measurements Lab (Van).

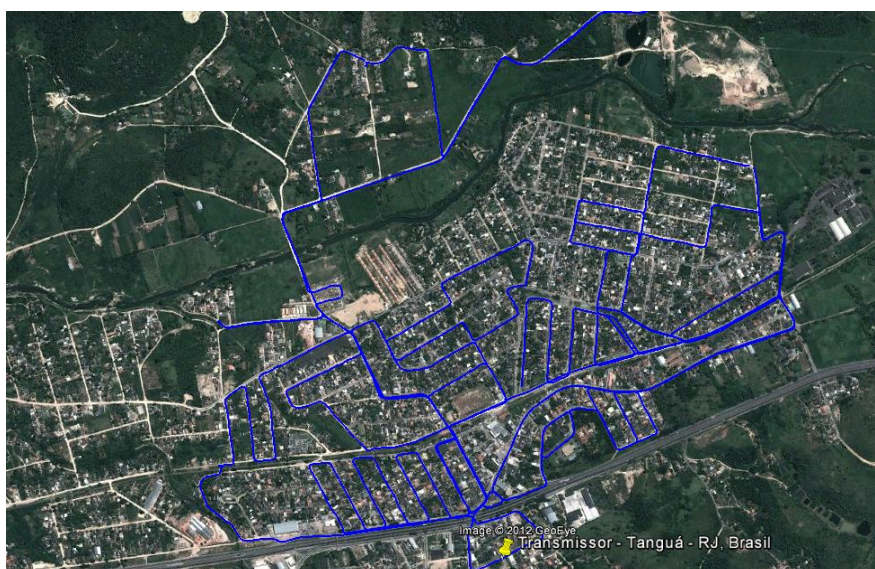


Fig. 3. Aerial view of the measured area and sounded routes. (Source: Google Map)

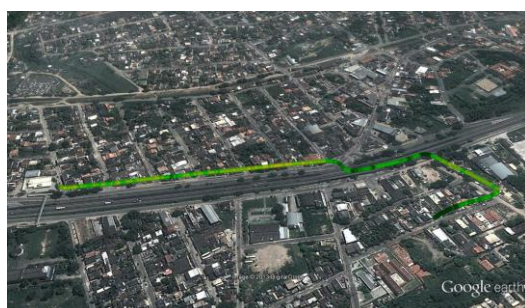


Fig. 4. Aerial view of Route 1 and Route 2.

III. NARROWBAND CHARACTERIZATION

A. Small scale statistics

For searching the narrowband statistics of the channel in the sounded frequency, a 5.765 GHz CW with 3 dBm level was transmitted to the power amplifier (PA) with a 28 dB gain and the signal was radiated. Cable and coupling losses were 15 dB approximately. In an average speed of 30 km/h, the mobile reception system acquired the signal at a 20 KSPS acquisition rate, saving it for offline processing.

1. Fading

Sectors of 40λ [8] length were taken in order to study the small scale variability of the signal. The mean signal level in each sector was calculated for studying the large scale variability and then, the path loss and the signal coverage were determined in the sounded area. Table II presents the number of sectors taken in the sounded routes and also provides the number of sectors that had the signal level effectively over the noise threshold and named filtered sectors. It is observed that the Route 7 had only one sector with signal level above that while the measured signal was totally below that in the Route 8 and so, this sector was discarded.

TABLE II. ROUTES, SECTORS AND ENVIRONMENT CHARACTERISTICS

Route	Sectors/Route	Filtered sectors
1	410	410
2	2347	1509
3	295	295
4	1398	764
5	1674	1047
6	935	270
7	1398	1
8	1012	0
9	1569	503
10	1549	1069
11	2295	1267

Even though a 33 dB gain LNA was used in the reception, the environment noise proved high enough to provide observable sectors on the farthest routes.

In each sector, probability density functions (p.d.f.) as Gauss [9], Rice [9], Rayleigh [9], Nakagami [9] and α - μ [10] were adjusted to the measurements in order to identify the one of best fitting to the environment considered. Figure 5 shows an example for the sector 155 in the Route 1. In it, Rayleigh is visibly the worst fitted p.d.f. and this occurred in the most of the sectors, as it is observed from Table III that provides the number of sectors that adjusted to each p.d.f. cited above.

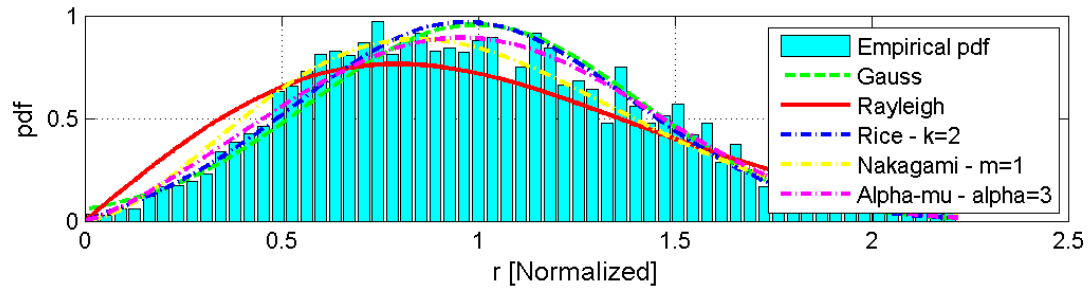


Fig. 5. P.d.f.s fitted to the data in the Sector 155/Route 1.

Among the p.d.f.s used, α - μ showed to have the smallest qui-squared error, in general, adjusting better to the small scale fading and it was followed by Gauss. The first has shown a good fitting to the small fading statistics in different channels like that through vegetation [11] in urban park and in land-air links in an aeronautical channel [12]. Rayleigh p.d.f. showed to be the worst fitting and Rice fits well in part of the sectors with high values for the k factor, in general. It is remembered that the Gauss p.d.f. is a limit of the Rice p.d.f. when k factor tends to infinity.

TABLE III. NUMBER OF FILTERED SECTORS THAT FITTED TO THE PDF'S

Route	Gauss	Rayleigh	Rice	Nakagami	α - μ
1	64	9	63	25	252
2	194	22	95	63	1151
3	33	10	46	17	197
4	58	5	35	14	656
5	129	7	46	30	835
6	69	0	19	0	179
7	0	0	0	0	1
9	73	10	55	53	320
10	146	7	87	33	802
11	131	6	118	35	982

2. LCR and AFD

Starting from the statistics, the level cross rate (LCR) and the average fade duration (AFD) were calculated for all the filtered sectors and Figure 6 provides an example that shows these parameters adjusted to the experimental data related to the sector 155 in the Route 1, the same characterized in Figure 5. It shows that the signal variability is large around the rms value and this is confirmed in most of the sectors. In this example, the normalized LCR is in the range 0.08 to 1, i.e., the envelope crosses the rms value in a range from 12.6 to 162 crossings while the normalized AFD is from 3×10^{-4} to 0.2, meaning 1.3 to 90 wavelengths for the average fading, both well fitted to Rice channel for this sector. It is worth observing that the car speed that carried the reception system was 30 km/h in most of routes, except in Route 2 in which it was 70 km/h.

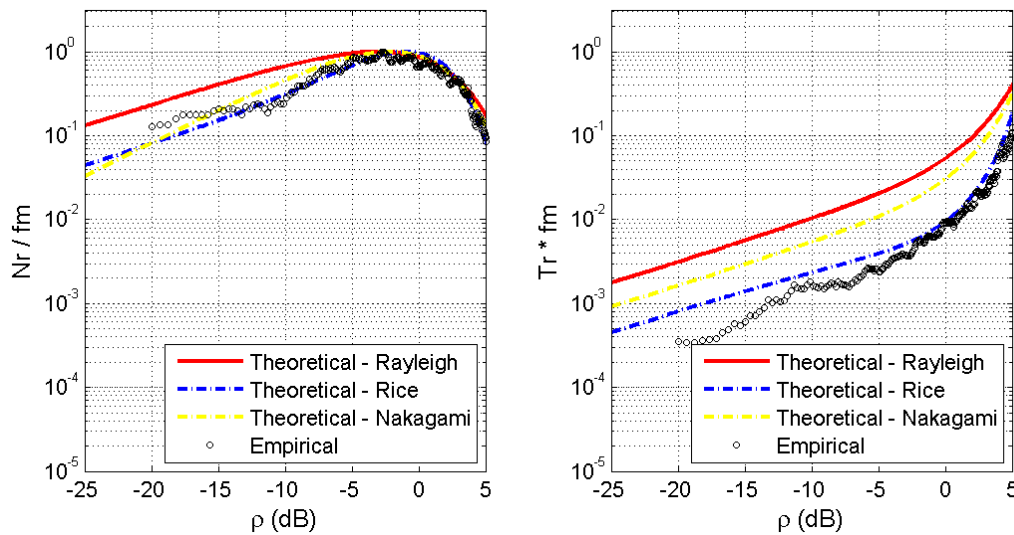


Fig.6. LCR and AFD fitted to the data for the Sector 155/Route 1.

B. Large scale statistics

1. Fading

An experimental probability density function (p.d.f.) was adjusted for the large scale variability of the signal taken as the signal mean in the sectors. Lognormal was the distribution best fitted to it, in all the routes, and Figure 7 shows an example for the Route 1. In Table IV the standard deviation of the distribution is presented, which is an important parameter using further in the SUI coverage prediction model and that varies in the 6.0 to 8.2 dB range [13]. It is observed that Route 7 has only one sector, so a unique mean and no histogram is possible to plot.

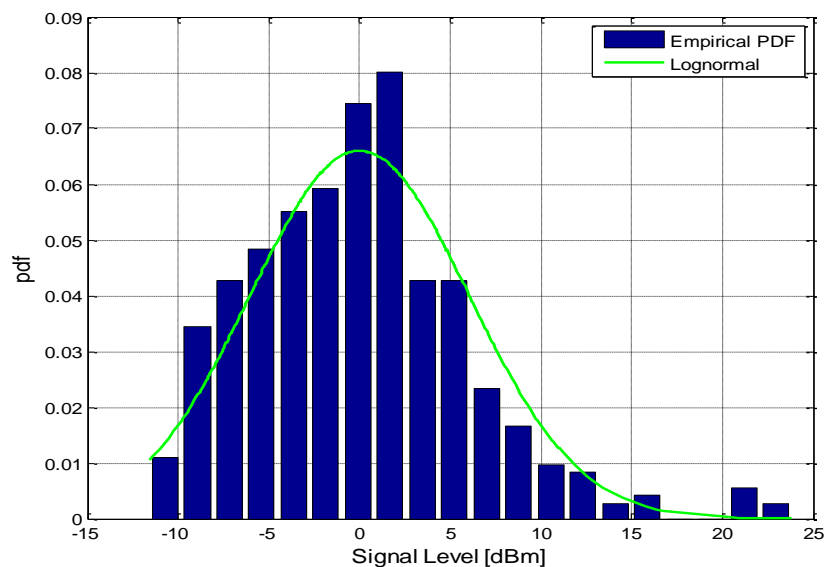


Fig. 7. Lognormal p.d.f. fitted to the large scale fading in the Route 1.

TABLE IV. STANDARD DEVIATION OF THE LOGNORMAL P.D.F.

Route	Std. deviation (dB)	Route	Std. deviation (dB)
1	6.0430	6	8.1193
2	6.4574	7	not applied
3	8.2270	9	7.4272
4	8.3303	10	6.7757
5	7.6520	11	6.7757

2. Path loss and coverage

For extracting the path loss from the long term fading, in logarithmic scale of distance as shown in Figure 8, a straight line was adjusted to it by using the MMSE (Minimum Mean Square Error) method and then, the attenuation factor could be determined for all routes and they are in Table V.

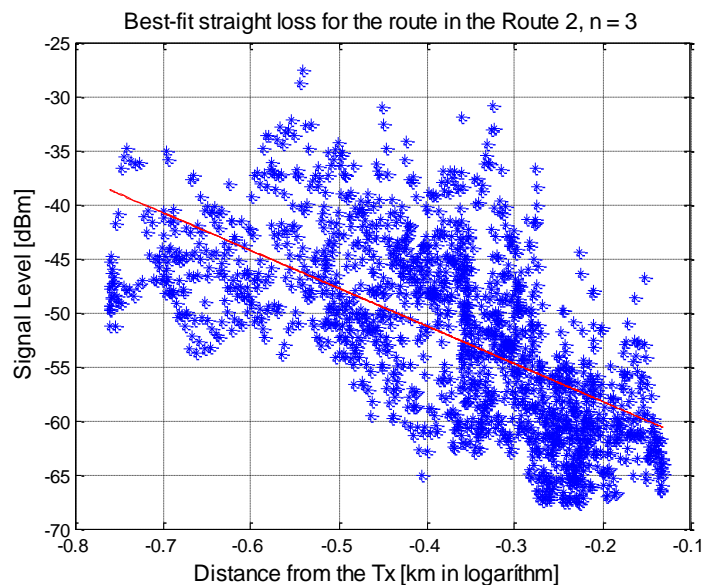


Fig. 8. Path loss fitted to the large scale fading in the Route 2.

TABLE V. ATTENUATION FACTOR FOR THE ROUTES

Route	Attenuation factor (α)	Route	Attenuation factor (α)
1	1	6	≈ 0
2	3	7	not applied
3	2	9	6
4	3	10	3
5	4	11	3

It is observed that Route 9 presents the highest attenuation factor (equal to 6) due to the terrain elevation and strong vegetation on that area contributing for the fast decrease of the signal.

For the coverage of the signal, three prediction models were used and they are summarized below.

- *Extended Hata-COST231*

This model is based on *Okumura-Hata model* with some changes to extend it until 6 GHz [14]-[15]. The median path loss is calculated as:

$$A_{\text{prop}} = 46.3 + 33.9 \log f - 13.82 \log h_b + (44.9 - 6.55 \log h_b) \log d - a(h_m) + C_m \quad (1)$$

$$a(h_m) = [1,1.\log f - 0,7].h_m - [1,56.\log f - 0,8] \tag{2}$$

where f is the frequency, in MHz; h_b is the transmission antenna height, in m; h_m is the receiving antenna height, in m; d is the distance between the Tx (Transmitter) and the Rx (Receiver) and C_m is null for suburban area, and 3 dB for urban area.

- *SUI*

The SUI (Stanford University Interim) model [16] gives the path loss equation and it is based on Erceg model with correction terms for the frequency and the Rx height. The path loss is given by:

$$A_{prop} = A_m + \Delta A_{prop_f} + \Delta A_{prop_h} \tag{3}$$

$$A_m = [B + 10(a - bh_b + c/h_b) \log(d/d_0)] + s \tag{4}$$

$$B = 20 \log(4\pi d_0/\lambda) \tag{5}$$

$$\Delta A_{prop_f} = 6 \log(f_{MHz}/ 2000) \tag{6}$$

$$\Delta A_{prop_h} = - 10.8 \log(h_b/2) \tag{7}$$

The parameters a , b and c are tabled according to the terrain category. Here, we have considered only b or c , in which: $a = 3.6$, $b = 0.005$ and $c = 20$. The variable d is the distance Tx-Rx and $d_0 = 100$ m; s is the standard deviation of the lognormal p.d.f. in dB adjusted to the large scale fading; h_b is the transmission antenna height, in m, and f is the frequency in MHz.

- *UFPA*

Starting from measurements carried out in Pará State, Brazil, a model was developed [7] suitable for environment with vegetation characteristic of this State. The final equation for the path loss is:

$$L = K_1 \log d + K_2 \log f + K_0 \tag{8}$$

where d is the distance Tx-Rx, in meters; f is the frequency, in MHz; K_1 and K_2 are parameters obtained with linear least squares; and K_0 is a correction factor expressed by:

$$K_0 = a - bX \tag{9}$$

The parameters a and b are adjusted by linear least squares and X is calculated as:

$$X = (H_1 + H_2)\lambda / (0.1 H_{OB}) \tag{10}$$

where H_1 and H_2 are, respectively, the Tx and Rx antenna height; λ is the wavelength; and H_{OB} is the average obstructions height.

Table VI presents a comparison of the error calculated for the fittings in each sounded route. Models SUI and UFPA have presented a better fit overall and, for a kind of environment like this we recommend the use of UFPA. [13].

TABLE VI. COMPARISON BETWEEN THE MODELS

Route	Model	Mean error	Std. deviation	RMS error
1	UFPA	2.8751	6.2113	6.8444
	SUI (B)	17.6366	14.7186	22.9715
	Cost231-Hata	32.8722	6.6305	33.5343
2	UFPA	5.6250	7.0484	9.0178
	SUI (B)	8.4469	6.8349	10.8658
	Cost231-Hata	34.3789	6.8477	35.0543
3	UFPA	0.0018	8.3148	8.3148
	SUI (B)	3.7524	9.1287	9.8698
	Cost231-Hata	29.0468	8.2525	11.8109
4	UFPA	6.8107	8.3996	10.8138
	SUI (B)	-0.284	8.4029	8.4077
	Cost231-Hata	8.3874	8.3347	11.8244
5	UFPA	4.0236	8.1957	9.1301
	SUI (C)	1.1792	7.7339	7.8233
	Cost231-Hata	5.9153	7.6564	9.6754
6	UFPA	3.6085	8.1553	8.9180
	SUI (C)	0.3050	8.4635	8.4690
	Cost231-Hata	5.8182	8.3196	10.1522
9	UFPA	1.1035	9.2353	9.3010
	SUI (B)	3.5478	7.5447	8.3372
	Cost231-Hata	29.9213	8.9758	31.2386
10	UFPA	3.4269	7.2828	8.0488
	SUI (C)	-0.3891	9.1154	9.1237
	Cost231-Hata	4.1019	7.4522	8.5066
11	UFPA	2.6408	7.9685	8.3947
	SUI (B)	-4.2234	15.4491	16.0160
	Cost231-Hata	30.3843	7.9172	31.3988

Figure 9(a) and Figure 9(b) show examples for Route 4 and Route 5, respectively, which compare the signal level predicted by the models with those experimental ones. In the SUI model the environment tested was classified as A (mountain terrain with moderate to high density of trees), B (plane terrain with moderate to high density of trees) and C (plane terrain with a light density of trees). In our environment the A category provided the bigger errors.

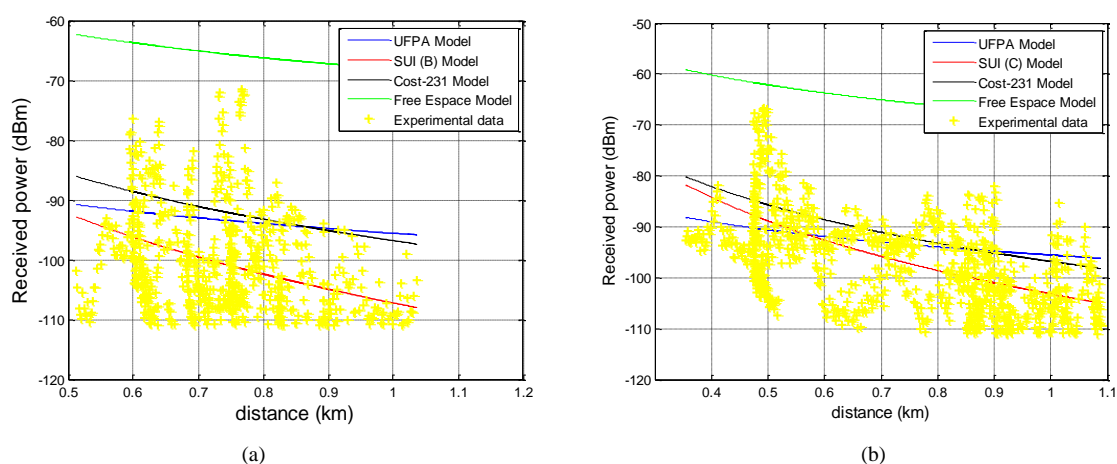


Fig. 9. Received signal and fitted models: (a) Route 4 and (b) Route 5.

IV. WIDEBAND CHARACTERIZATION

In the wideband sounding a 20 MHz OFDM code was generated in *Matlab*[®] as it is shown in Figure 10, and sent to the Vector Signal Generator for further radiation through the sectorial antenna. Receiving the signal with the Signature High Performance Signal Analyzer together the GPS data in a 50 MSPS rate, I and Q components of the signal and the position of the receiver were saved in files for offline processing. Before starting the GPS (Global Positioning System), its clock was synchronized to the internal clock of the Signature so that the mobile position and the signal amplitude were taken at the same time. As the GPS captures the position in 1 second intervals, it was possible to interpolate position data since the car speed was practically constant. It is important to say that the sounded environment was the same but the number of routes was different due to the smaller dynamic range of the wideband measurements.

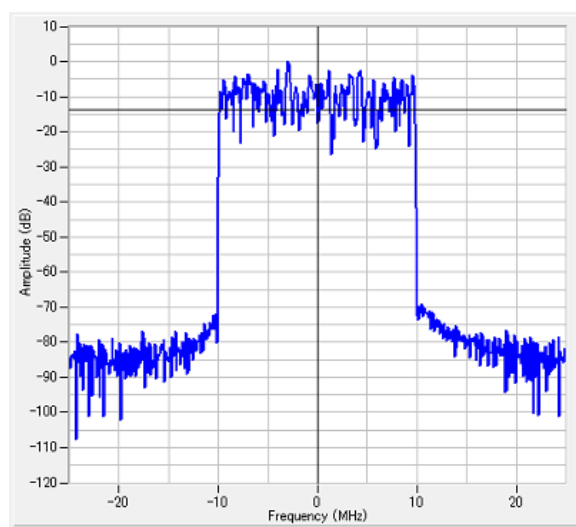


Fig. 10. OFDM signal used as test signal.

A. Small scale analysis

In wideband analysis the fading is largely seen as the channel behavior along the time and the time dispersion of the signal, which is characterized by the delay spread and the coherence band. Then, in small scale they are calculated for each response in time/delay and time/frequency domain, respectively. From the acquired data and by using the matched filter technique in software, the power delay profiles (PDPs) were calculated by adequate data processing in order to result the time dispersion parameters as mean delay, delay spread and coherence band. However, before this processing, the PDPs were denoised with the WDEN (Wavelet Denoising) technique in order to identify the valid multipath. The *symlet8* functions have already proven good application to the PDPs and they were used separately to the real and imaginary parts of the PDPs [17]. Table VII provides the time dispersion parameters obtained in the sounded routes.

TABLE VII. TIME DISPERSION PARAMETERS

Route	Mean delay [μs]	Rms delay [μs]	Coherence band. [kHz]	Number of PDPs
1	0.0924	1.3842	60.8382	693
2	0.0673	0.8025	86.2658	312
3	0.0394	0.3469	100.2463	112
4	0.0591	0.8472	71.4315	440
5	0.0949	1.1558	55.0264	252
6	0.0869	1.1977	57.2796	240
7	0.0780	0.7516	107.8193	142
8	0.0517	0.7519	72.1443	337

It is observed that the delay spread is smaller in the Route 3, which presents LOS to the Tx antenna and strong signal, as it is seen in Figure 11. In more distant routes it varies in the 0.75 - 1.38 μs range and the vegetation and buildings contribute a lot for the bigger values such as those calculated for Routes 5 and 6. It is observed in Figure 12 (a), for the Route 1, that the relation between the delay spread and the coherence bandwidth is not a constant as has found Rappaport [18] in a particular channel. Then, the transmission rate is variable and with strong predominance until 60 kbps in the Route 1, as it is observed from Figure 12(b) in which the 90% coherence bandwidth values are plotted for this route.

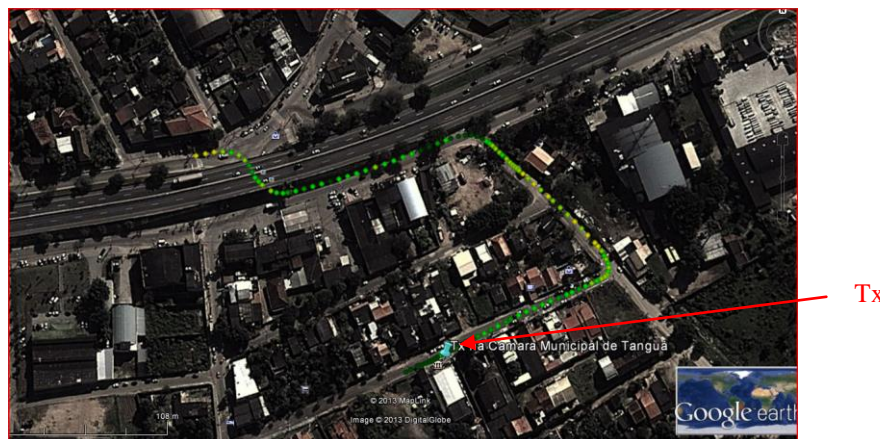


Fig. 11. Route 3 and the position of the transmitter.

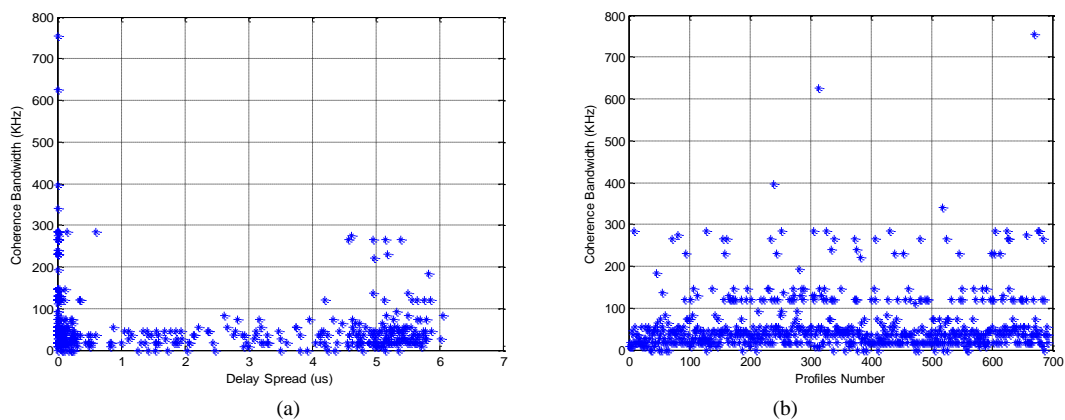


Fig. 12. Coherence bandwidth in the Route 1 versus: (a) delay spread and (b) profile number.

B. Large scale analysis

Since the channel stationarity is limited to small scale, when it is desired to determine the parameters for larger areas it is not possible to do directly from the correlation functions of the WSSUS channel [9]. So, when dealing with greater distances, the stationarity can only be guaranteed in pieces through the channel behavior in a small scale and in homogeneous small and adjacent areas. An analysis that covers each complete route is the calculus of the mean power of the OFDM signal received along the distance and a comparison of this wideband measurement is made with the coverage prediction models in order to test the models fitted to the data in the narrowband characterization of the channel. Table VIII provides the results and it is observed that the fitting error overcomes those obtained in the narrowband analysis, in general, but the SUI and UFPA prediction models keep the best adjustment to the experimental values.

TABLE VIII. COMPARISON BETWEEN THE MODELS IN WIDEBAND DATA

Route	Model	Mean Error	Std deviation	RMS Error
1	UFPA	6.995169	5.985115	9.206193
	SUI (A)	3.538532	7.703615	8.477434
	SUI (B)	5.637025	7.430649	9.326875
	SUI (C)	8.402019	7.264007	11.10674
	HCost231	12.0467	6.498952	13.68793
2	UFPA	3.90335	7.366751	8.336976
	SUI (A)	2.868867	22.32966	22.51319
	SUI (B)	4.765121	20.87867	21.41554
	SUI (C)	7.400022	19.9513	21.27944
	HCost231	10.33081	14.98727	18.20285
3	UFPA	5.29307	7.298524	9.015822
	SUI (A)	30.67912	17.01834	35.08322
	SUI (B)	30.36939	15.87915	34.27021
	SUI (C)	31.58525	15.15745	35.03393
	HCost231	26.72897	11.42996	29.07029
4	UFPA	8.328168	5.244329	9.841817
	SUI (A)	9.063299	6.806017	11.33425
	SUI (B)	10.8118	6.507134	12.61895
	SUI (C)	13.35165	6.325745	14.77436
	HCost231	15.76087	5.520219	16.69964
5	UFPA	5.091191	6.70981	8.422694
	SUI (A)	-3.86879	6.561155	7.616842
	SUI (B)	-1.31079	6.547449	6.67737
	SUI (C)	1.749784	6.541152	6.771146
	HCost231	7.016495	6.541913	9.593114
6	UFPA	7.921083	6.978229	10.55648
	SUI (A)	2.995554	6.879726	7.503597
	SUI (B)	5.216692	6.859706	8.617972
	SUI (C)	8.06058	6.849533	10.57776
	HCost231	12.1382	6.831753	13.9287
7	UFPA	8.017318	6.366559	10.2377
	SUI (A)	-0.7886	5.326978	5.385033
	SUI (B)	1.756533	5.30182	5.585222
	SUI (C)	4.808836	5.297243	7.154417
	HCost231	10.03014	5.432827	11.40698
8	UFPA	7.849975	6.436107	10.15114
	SUI (A)	7.566075	10.18157	12.68503
	SUI (B)	9.39966	9.610577	13.4431
	SUI (C)	11.99425	9.25642	15.15069
	HCost231	14.70381	7.563506	16.53507

V. CONCLUSION

The Brazilian Government develops a program known as *Digital City* which provides free internet access for the population, and they are using the unlicensed band of 5 GHz with WiMAX technology. Therefore, it is important to study the signal coverage on this band to provide channel data to the operators in order to allow them reach a good coverage planning. Besides this, the determination of some wideband parameters is important to choose, for example, the appropriate data transmission rate in this kind of environment.

Brazilian people live majorly in suburban areas for which little, or even none, channel characterization exists. Hence, this work try to fill this lack of information to help planners to do a better project. Thus, starting from measurements on the 5.765 GHz band in Tanguá city, Rio de Janeiro (a suburban environment), the large scale fading was estimated for several routes and then, the path loss was determined. In the following step, some prediction models, applied to this band, were used in order to predict the signal level in this area. By comparing these values with the experimental ones, among the models used, those that can better predict the signal level in such environment are: UFPA, SUI and, at last, the Extended Hata-COST231 model. The same occurred with the OFDM wideband signal. In the routes where the UFPA model was not the best, it presented an error slightly larger than the SUI model. However, the Extended Hata-COST231 did not fit, in general, leading to larger errors. It is worth to observe that Tanguá city resembles, in many aspects, the city where the measurements for generating the UFPA model were carried out. Then, UFPA model showed to be an appropriate model for predicting the mean signal level in suburban areas with some kind of vegetation.

From the statistical analysis of fading, it is observed that the channel has behaved as α - μ distribution in general, followed by gaussian or rician with high k factor indicating the tendency to gaussian. The level cross rate (LCR) and average fade duration (AFD) show that the signal variability is large around the rms value and this is confirmed in most of the sectors. This implies that, although the signal has a good level, there is the possibility of deep fading, which can fail the communication, due to the multipath acting not only for enhancing the signal level but also reducing it. Several techniques help to get round this fading. The use of rake receiver is one of them.

The wideband parameters show that delay spread and coherence bandwidth vary, respectively, from 0.34 to 1.38 μ s and 55.03 to 107.82 kHz, indicating that the transmission rate in this channel is limited to hundreds of kbps and the equalization is necessary for desired larger rates. MIMO (Multiple In Multiple Out) system and appropriate modulation are techniques which can be used to increase this rate.

The extensive data array obtained from the measurements permitted to understand the suburban channel behaviour, typical of those used in the *digital cities* of Brazil, and to determine the main

parameters, providing results that are mainly useful to the planners in order to improve the signal coverage on this kind of environment and the data transmission rate.

ACKNOWLEDGMENT

To CNPq for the scholarship allowed to one of the authors and to INCT-CSF Project for the financial support.

REFERENCES

- [1] ANATEL, “Plano de Atribuições, Destinação e Distribuição de Frequências no Brasil”, pp. 178, 2011.
- [2] Alam, D. and Khan, R. H., “Comparative Study of Path Loss Models of WiMAX at 2.5 GHz Frequency Band”, Int. Journal of Future Generation Communication and Networking, vol. 6, N. 2, pp. 11-23, April 2013.
- [3] Boutin, M., Affes, S., Despins, C; Denidni, T., ”Statistical Modelling of a Radio Propagation Channel in an Underground Mine at 2.4 and 5.8 GHz”, IEEE Vehicular Technology Conference, 2005, VTC-2005-Spring , vol. 1, pp. 78 – 81, IEEE.
- [4] Fonseca, F. J. B. , Dias, P. P., Dal Bello, J. C. R. and Matos, L. J., “Variabilidade e Cobertura de Sinal Rádio Móvel na Faixa de 3,5 GHz em Ambiente Urbano”, 15º SBMO – Simpósio Brasileiro de Micro-ondas e Optoeletrônica 10º CBMag – Congresso Brasileiro de Eletromagnetismo MOMAG 2012, pp. 1-5, João Pessoa, PB, Brazil.
- [5] Shahajahan, M. and Hes-Shafi, A. Q. M. A., Analysis of Propagation Models for WiMAX at 3.5 GHz, PhD Thesis, Blekinge Institute of Technology, pp. 62, Sweden, Sep. 2009.
- [6] Castro, B. S. L., Modelo de Propagação para Redes sem Fio Fixas na Banda de 5.8 GHz em Cidades Típicas da Região Amazônica, Dissertação de Mestrado, UFPA, Belém, Brazil, pp. 58, 2010.
- [7] Vale, M. F., Gomes, I. R., Castro , B. S. L. , Barros, F. J. B. and Cavalcante, G.P.S., “New Terrain Proposal for SUI Model Equations Based on 5.8 GHz Measurements in Wooded Cities Found in Amazon Region”, 6TH European Conference on Antennas and Propagation Proceedings, pp 1187-1189, 26-30 March 2012, Prague.
- [8] Urie, A., “Errors in estimating local average power of multipath signals”, Electronic Letters, vol. 27, issue 4, pp.315-317, Feb 14th, 1991.
- [9] Parsons, J. D., The Mobile Radio Propagation Channel, John Wiley & Sons, 2nd. Ed., pp. 433, 2000.
- [10] Yacoub, M. D., “The α - μ distribution: a general fading distribution, Proc. IEEE Inter. Symp. on Personal, Indoor and Mobile Radio Com., vol. 2, pp. 629–633, Sep 2002.
- [11] Leão, E. S., Fonseca, F. J. and Matos, L. J., "Análise Estatística da Variabilidade do Sinal Rádio Móvel Medido em Ambiente de Vegetação", 15º SBMO – Simpósio Brasileiro de Micro-ondas e Optoeletrônica 10º CBMag – Congresso Brasileiro de Eletromagnetismo MOMAG 2012, pp. 1-5, João Pessoa, PB, Brazil.
- [12] Paiva, L. S. and Matos, L. J., “Statistical Analysis of the Radiomobile Signal in the 1140 MHz Band of an Aeronautical Channel”, Microwave & Optoelectronics Conference (IMOC), 2013 SBMO/ IEEE MTT-S International, pp. 1-5, Rio de Janeiro, RJ, Brazil, 4-7 Aug 2013.
- [13] Meza, W. D. T., Siqueira, G.L., Santos, M. A. G. and Matos, L. J., “Signal Coverage in a Suburban Area in the 5.8 GHz Frequency Band”, Microwave & Optoelectronics Conference (IMOC), 2013 SBMO/ IEEE MTT-S International, pp. 1-5, Rio de Janeiro, RJ, Brazil, 4-7 Aug 2013.
- [14] Blaunstein, N., Radio Propagation in Cellular Networks, Artech House Publishers, pp. 405, 1999.
- [15] Plitsis, G., “Coverage Prediction of New Elements of Systems Beyond 3G: The IEEE 802.16 System as a Case Study”, Proc. IEEE VTC 2003-Fall, Vol. 4, pp.2292-2296, Oct 2003.
- [16] J.G. Andrews, A. Gosh, and R.Muhammed, Fundamentals of WiMAX: Understanding Broadband Wireless Networking, Prentice Hall, pp. 449, 2007.
- [17] Dias, M.H.C. and Siqueira, G.L., “On the Use of Wavelet-Based Denoising to Improve Power Delay Profile Estimates from 1.8 GHz Indoor Wideband Measurements”, Wireless Personal Comm., pp.153-175, Springer 2005.
- [18] Rappaport, T. S., Wireless Communications: Principles and Practice, Prentice Hall PTR, 2nd Ed., pp. 163, 1996.